Journal of Experimental Botany, Vol. 64, No. 7, pp. 2005–2016, 2013
doi:10.1093/jxb/ert064 Advance Access publication 4 March, 2013
This paper is available online free of all access charges (see http://jxb.oxfordjournals.org/open_access.html for further details)

Journal of Experimental Botany
www.jxb.oxfordjournals.org

RESEARCH PAPER

Visualization and quantification of protein interactions in the biosynthetic pathway of molybdenum cofactor in *Arabidopsis thaliana*

David Kaufholdt, Christian Gehl, Mirco Geisler, Olga Jeske, Sabrina Voedisch, Christine Ratke*, Benjamin Bollhöner*, Ralf-R. Mendel and Robert Hänsch†

Institut für Pflanzenbiologie, Technische Universität Braunschweig, Humboldtstrasse 1, D-38106 Braunschweig, Germany
*Present address: Umeå Plant Science Centre, Department of Forest Genetics and Plant Physiology, Swedish University of Agricultural Sciences (SLU), S901-83 Umeå, Sweden.

† To whom correspondence should be addressed. E-mail: r.haensch@tu-bs.de

Received 11 December 2012; Revised 14 February 2013; Accepted 17 February 2013

Abstract

The molybdenum cofactor (Moco) is the active compound at the catalytic site of molybdenum enzymes. Moco is synthesized by a conserved four-step pathway involving six proteins in *Arabidopsis thaliana*. Bimolecular fluorescence complementation was used to study the subcellular localization and interaction of those proteins catalysing Moco biosynthesis. In addition, the independent split-luciferase approach permitted quantification of the strength of these protein–protein interactions *in vivo*. Moco biosynthesis starts in mitochondria where two proteins undergo tight interaction. All subsequent steps were found to proceed in the cytosol. Here, the heterotetrameric enzyme molybdopterin synthase (catalysing step two of Moco biosynthesis) and the enzyme molybdenum insertase, which finalizes Moco formation, were found to undergo tight protein interaction as well. This cytosolic multimeric protein complex is dynamic as the small subunits of molybdopterin synthase are known to go on and off in order to become recharged with sulphur. These small subunits undergo a tighter protein contact within the enzyme molybdopterin synthase as compared with their interaction with the sulphurating enzyme. The forces of each of these protein contacts were quantified and provided interaction factors. To confirm the results, *in vitro* experiments using a technique combining cross-linking and label transfer were conducted. The data presented allowed the outline of the first draft of an interaction matrix for proteins within the pathway of Moco biosynthesis where product–substrate flow is facilitated through micro-compartmentalization in a cytosolic protein complex. The protected sequestering of fragile intermediates and formation of the final product are achieved through a series of direct protein interactions of variable strength.

Key words: Bimolecular fluorescence complementation, molybdenum cofactor biosynthesis, protein cross-linking, protein–protein interaction, *Rhizobium* infiltration, Split-luciferase.

Introduction

The transition element molybdenum (Mo) is an essential micronutrient for plants, animals, and most microorganisms (Schwarz and Mendel, 2006). The metal itself is biologically inactive unless it is complexed by a specific cofactor. With the exception of bacterial nitrogenase, Mo is bound to a pterin, thus forming the molybdenum cofactor (Moco) which is the active compound at the catalytic site of all other Mo enzymes.

Abbreviations: BiFC, bimolecular fluorescence complementation; Cnx, cofactor for nitrate reductase and xanthine dehydrogenase; cPMP, cyclic pyranopterin monophosphate; FluCI, floated-leaf disc luciferase complementation imaging; Moco, molybdenum cofactor, MPT, molybdopterin.

In plants, there are five Mo-enzymes (for reviews, see Bittner and Mendel, 2010; Mendel and Kruse, 2012): (i) nitrate reductase catalyses the key step in inorganic nitrogen assimilation; (ii) aldehyde oxidase is essential for the biosynthesis of the phytohormone abscisic acid; (iii) xanthine dehydrogenase is involved in purine catabolism and reactive oxygen production; (iv) sulphite oxidase detoxifies excess sulphite; and (v) mitochondrial amide oxime reducing component is probably involved in detoxifying reactions.

In all organisms studied so far, Moco is synthesized by a conserved biosynthetic pathway that can be divided into four steps, according to its biosynthetic intermediates (Fig. 1). Six proteins have been identified to catalyse Moco biosynthesis in plants (for reviews, see Schwarz *et al*., 2009; Mendel and Kruse, 2012). In the first step, 5'-GTP is converted to cyclic pyranopterin monophosphate (cPMP; Hänzelmann *et al*., 2002; Santamaria-Araujo *et al*., 2004). In the second step, a dithiolene group is introduced into cPMP by transfer of two sulphur atoms whereby molybdopterin (MPT) is formed. This reaction is catalysed by the enzyme MPT synthase, a heterotetrameric complex consisting of two large Cnx6 and two small Cnx7 subunits. After MPT synthase has transferred the two sulphurs to cPMP, it has to be re-sulphurated by the MPT synthase sulphurase (Matthies *et al*., 2004). In the third step (Fig. 1), MPT is bound by the protein molybdenum insertase Cnx1 and becomes activated by adenylation, thus forming MPT-AMP (Kuper *et al*., 2004). During the fourth and final step, MPT-AMP is transferred from the G-domain to the E-domain of Cnx1 where the adenylate is cleaved and Mo is inserted, finally yielding mature Moco (Llamas *et al*., 2006).

With the exception of sulphite oxidase (Nowak *et al*., 2004) and mitochondrial amide oxime reducing component (Havemeyer *et al*., 2006; unpublished data), all remaining plant Mo enzymes are located in the cytoplasm. This may be taken as an indication that at least the last step of Moco biosynthesis also proceeds in the cytoplasm. Recently Teschner *et al*. (2010) have shown that the first step of Moco biosynthesis localizes to mitochondria that export the intermediate cPMP to the cytoplasm. Therefore, it became of interest to study where the remaining steps of Moco biosynthesis take place. From another point of view, this question became imperative as both biosynthesis intermediates cPMP and MPT are labile in solution and need protection (Wuebbens and Rajagopalan, 1993). Hence, it would be exceedingly unlikely that MPT as the product of step two is simply released by MPT synthase (compare Fig. 1) and diffuses as free MPT to Cnx1 that converts it into mature Moco. Therefore, the existence of a multienzyme complex was discussed (Mendel and Bittner, 2006) that facilitates product–substrate flow, which could result in micro-compartmentalization through a hypothetical Moco biosynthetic multienzyme complex. This would ensure a swift and protected transfer of the labile intermediates within the reaction sequence from GTP to Moco. After establishing that cPMP was exported from the mitochondria to the cytoplasm (Teschner *et al*., 2010), it was deemed of importance to determine (i) whether the enzymes that convert cPMP to Moco (i.e. MPT synthase and Cnx1) are localized in the cytoplasm; and (ii) if there is a protein–protein interaction between them. Even a weak and transient contact between both proteins should be sufficient to transfer the highly labile MPT from MPT synthase to Cnx1.

Powerful tools are available to answer these questions. Bimolecular fluorescence complementation (BiFC) (Kerppola, 2008; Gehl *et al*., 2009) permits both localization and checking for protein interaction within a living cell. The disadvantage of BiFC is that it is not dynamic and gives only a yes or no answer. Here another *in vivo* approach is very helpful: the Split-luciferase (Split-LUC) approach permits the study of dynamic protein interactions as the LUC termini are not covalently bound upon interaction, thereby enabling the quantification of complex formation (Luker *et al*., 2004; Chen *et al*., 2008). The enzymatic activity of reconstituted LUC correlates directly with the stability and strength of protein–protein interactions. Recently, this approach was combined with an improved floated-leaf disc assay. In this process, the leaf is infiltrated with a luciferin solution through stomatal openings, thus enabling investigation of protein interactions directly in intact leaf tissue discs using a luminometer (Gehl *et al*., 2011). Other tools to uncover protein–protein interactions are the *in vitro* approaches. They have the advantage of measuring interactions between purified proteins in a defined system. An improved system of protein cross-linking was utilized where a novel trifunctional linker (Layer *et al*., 2007) allows observation of label transfer between interacting proteins *in vitro*. Using all three approaches one can deduce that the conversion of cPMP to Moco involves a cytosolic complex probably consisting of at least six protein subunits that belong to two different multimeric enzymes.

Materials and methods

Generation of GATEWAY expression vectors and in planta *transformation*

All molecular techniques were performed using standard protocols (Sambrook and Russell, 2001). The GATEWAY cloning technology (Invitrogen, http://www.invitrogen.com) was used, providing an easy and efficient way to clone every gene of interest into destination vectors for localization (Supplementary Table S1 available at *JXB* online), BiFC (Gehl *et al*., 2009), and floated-leaf luciferase complementation imaging (FLuCI) (Gehl *et al*., 2011). In all expression vectors, flexibility between the reporter and fused protein of interest is realized by a peptide linker which is shown in Supplementary Table S2.

The cDNAs from *Arabidopsis thaliana* full-length *cnx1* (AT5G20990), the *cnx1E* and *cnx1G* domains (according to Stallmeyer *et al*., 1995), *cnx2* (AT2G31955), *cnx3* (AT1G01290), and *cnx5* (AT5G55130) were cloned into the donor vector pDONR/Zeo using the GATEWAY BP reaction system to create entry vectors, with and without a final stop codon. Moreover, mutations of the C-terminus of Cnx7 were created by using specific primer sets. The primers used are listed in Supplementary Table S3 at *JXB* online. These entry vectors were used to create the final expression constructs by LR reaction (Invitrogen), producing the GATEWAY expression vectors for localization, BiFC, and FLuCI. All vectors were provided with a selection marker for kanamycin in *Escherichia coli* and *Rhizobium tumefaciens*. The *Cauliflower mosaic virus* (CaMV) 35S promoter was used to drive gene expression. All produced or already published constructs cited herein are listed in Supplementary Tables S1, S4, S5. The expression constructs were introduced into *R. tumefaciens* strain C58C1/pMP90 via electroporation.

After transferring the binary vectors into *R. tumefaciens* C58C1, the fusion gene constructs were (co-)transferred by

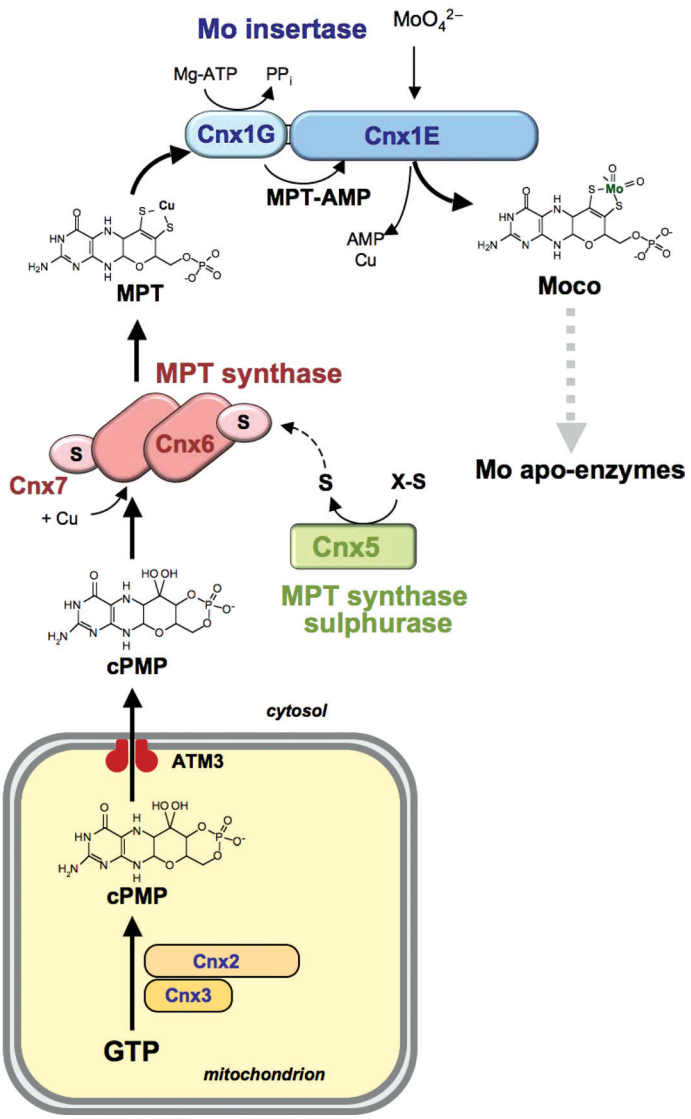

Fig. 1. Biosynthesis of Moco in plants. The pathway of Moco synthesis can be divided into four steps. The intermediates and the names of the Moco biosynthesis enzymes are given. Step 1: biosynthesis starts with conversion of GTP to cPMP in the mitochondria. The transporter ATM3 is involved in export of cPMP to the cytosol. Step 2: heterotetrameric MPT synthase, consisting of Cnx6 and Cnx7, inserts two sulphur atoms into cPMP and converts it to MPT. MPT synthase receives the sulphur from Cnx5 (MPT synthase sulphurase), with the primary sulphur donor of Cnx5 (X-S) being unknown. It is assumed that copper (Cu) is inserted directly after dithiolene formation. Step 3: MPT is adenylated by the Cnx1 G-domain of Mo insertase Cnx1, thus forming MPT-AMP. Step 4: MPT-AMP is transferred to the Cnx1 E-domain where Mo is inserted by replacing Cu, thus forming Moco which is finally allocated to Mo apo-enzymes. For better readability, the colours used for drawing the respective enzymes are the same in all figures and in Table 1.

Rhizobium-infiltration into leaf cells of *Nicotiana benthamiana*. In order to increase continuity for cohesive results, the Rhizobium-infiltration was completely standardized, most notably for the culture time of *R. tumefaciens*, the optical density, and the induction by acetosyringone (for details, see Gehl *et al*., 2009, 2011). For direct comparison of both the interaction approach and the specific negative control, one half of the same leaf was infiltrated with an identical concentration of *R. tumefaciens*. The results shown were derived from 10–16 leaves, produced from 3–4 plants, originating from 2–3 independent transformation events. Between 3 d and 5 d after infection, luminescence and fluorescence, respectively, were monitored.

Quantification of protein–protein interaction using split LUC

Luminescence was quantified in *N. benthamiana* using FluCI (Gehl *et al*., 2011). One half of a previously transformed leaf was cut off and infiltrated with a FLuCI solution before punching six discs of 12 mm diameter for measurement. Emitted photons were detected by a luminometer (TriStar multimode reader, Berthold Technologies www.berthold.com) using a multiwell plate (24-well format) for 20 min after luciferin infiltration. The peak luminescence represents the LUC value for the single leaf disc. Simultaneously, a plate and a negative control were tested for the constructs of interest which contain one of the analysed constructs and a neutral non-interacting control construct. After luminescence measurement, leaf discs of each approach were pooled to be frozen in liquid nitrogen and stored at -75 °C for β-glucuronidase (GUS) calibration.

GUS assay (Jefferson *et al*., 1987) was used to compare different expression levels in the two leaf halves of the interaction approach and the negative control for calibration of the luminescence values with each other. Therefore, a GUS expression vector was co-infiltrated together with all approaches at an equal concentration. GUS assay was performed as described earlier (Gehl *et al*., 2011). Fluorescence was detected by TriStar multimode reader (Berthold Technologies). The GUS values were adjusted to the analysed protein concentration according to Bradford (1976).

The split LUC factor was calculated according to Gehl *et al*. (2011). It describes the quotient (named Q1) between the arithmetic means of LUC values of the interaction approach and the direct negative control – each derived from six independent leaf discs of one leaf half. Differences in GUS expression were used to calibrate the LUC values. Moreover, the difference in protein abundance in the cell has to be taken into account as it turned out that the unspecific background fluorescence (i.e. the unspecific reconstitution of the two LUC halves) was dependent on the protein concentrations of the two halves. Therefore, FLuCI assays of the following protein pairs have to be performed: (i) 'A+B'=the two proteins of interest; and (ii) 'A+negative control' is tested with a protein that shows no interaction with A, thus giving the background fluorescence. However, as it is possible that protein A is expressed more strongly or more weakly than the negative control, the abundance of both has to be determined. Therefore, protein A and the negative control have to be checked against another independent control protein C, interacting neither with A nor with the negative control. Hence two more FLuCI assays have to be performed: (iii) 'A+C' and (iv) 'negative control+C'. The quotient (named Q2) of these LUC values correlates with the variation of protein abundance in the cells. For this purpose, the Venus^{N137}–CLUC fusion construct was created, which could be used in both split protein assays. Finally, the quotient between Q1 and Q2 defines the split LUC factor.

Microscopic detection for localization and BiFC interaction studies

The cLSM-510META scanhead connected to the Axiovert 200M (Carl Zeiss, http://www.zeiss.de) was used to visualize the fluorescence in the lower epidermis of leaf discs as described by Gehl *et al*. (2009). For BiFC interaction studies, several representative pictures from 5–10 leaf discs of 2–3 plants were taken with identical microscope settings for (i) the proteins of interest approach; (ii) the negative control; and (iii) the respective abundance control. In analogy to the FLuCI assay, the abundance control was an additional BiFC

assay to estimate the different concentrations of the negative control protein relative to its counterpart in the interaction study by using a second independent reporter–protein construct. The spectral signature was detected in the lambda mode of the most fluorescing quarter of the recorded picture.

Cross-linking and biotin label transfer

Proteins used for *in vitro* interaction experiments were cloned into pQE80 (Qiagen, http://www.qiagen.com), overexpressed in the *E. coli* strain DL41, and purified using Ni-NTA agarose as described by Kruse *et al*. (2010). Cross-linking experiments were carried out as described by Kruse *et al*. (2010).

Protein extraction, western blot, and immunodetection

Plant material (100 mg) was squeezed and sonicated at 4 °C in 100 µl of extraction buffer (100 mM potassium phosphate, pH 7.5; 5 mM dithiothreitol; 2 mM EDTA), followed by centrifugation at 22 000 *g* (4 °C, 10 min). Protein concentration was determined according to Bradford (1976) with bovine serum albumin (BSA) as protein standard.

For immunodetection, 50 µg of protein was separated by 7.5% SDS–PAGE and transferred to a nitrocellulose membrane (Hybond-P, GE Healthcare, http://www.gehealthcare.com) by electroblotting. The primary antibody against the green fluorescent protein (Living Colors® Full-Length A.v. Polyclonal Antibody, Clontech, www.clontech-europe.com) was diluted 1:500 prior to use. The detection was accomplished with alkaline phosphatase-conjugated anti-rabbit antibody (Sigma, http://www.sigmaaldrich.com) and stained with BCIP/NBT (according to the manufacturer's instructions, Promega, http://www.promega.com).

Results

Protein interaction between the subunits of molybdopterin synthase

Once the intermediate cPMP is formed and exported from the mitochondria to the cytosol, it becomes converted to MPT in step 2 of Moco biosynthesis (compare Fig. 1; Supplementary Fig. S1 at *JXB* online). This reaction is catalysed by MPT synthase, a heterotetrameric complex of two large Cnx6 subunits (22.2 kDa) and two small Cnx7 subunits (10.5 kDa) (Fig. 1). Previously it was demonstrated that Cnx6 dimerizes and that Cnx6/Cnx7 show heterodimerization (Gehl *et al*., 2009). These BiFC results were quantified in the newly described split LUC complementation assay by transiently expressing the constructs in *N. benthamiana* as described by Gehl *et al*. (2011). Here the controls are of particular importance. (i) Transformation efficiency was calibrated via additional GUS expression. (ii) The LUC values measured were corrected by a protein abundance factor in order to take into account that unspecific background fluorescence is dependent on the expression level of both the protein to be tested and the negative control (for details, see the Materials and methods). The results are given in Table 1A (for better readability, the boxes in Table 1 are coded in the same colour as the respective proteins in all figures). The values measured show that the binding strength of Cnx6/Cnx6 pair (split LUC factor 12.0 ± 3.0) is as strong as heterodimerization between Cnx6 and Cnx7 (11.9 ± 4.5).

Protein interaction between molybdopterin synthase and molybdopterin synthase sulphurase

The heterotetrameric protein complex of MPT synthase is dynamic as during its reaction cycle the two small Cnx7 subunits have to go on and off to become recharged with sulphur by the enzyme Cnx5 (compare Fig. 1), which is designated as MPT synthase sulphurase (Mendel and Schwarz, 2011). Therefore, the two subunits of MPT synthase as well as the sulphurase Cnx5 were tested in the split LUC complementation assay. The N-terminal half of luciferase (=NLUC) was fused to the N-terminus of Cnx5 (giving NLUC–Cnx5) and the C-terminal half of luciferase (=CLUC) was fused to the N-terminus of Cnx7 (giving CLUC–Cnx7). Based on in total >90 samples derived from ≥15 leaves, a split LUC factor was calculated including GUS calibration and the protein abundance factor. Supplementary Fig. S2 and Supplementary Tables S6 and S7 at *JXB* online show these results for leaves derived from four plants. For each plant, values of four infiltrated leaves are given in order to demonstrate variation between leaves and between plants. A factor >1.0 means interaction; ≤1.0 represents no interaction depending on the given standard deviation, thus showing that luminescence was caused non-specifically by accidental contact. No interaction was measurable when the sulphurase Cnx5 was tested in combination with Cnx6 (Supplementary Fig. S2A; Supplementary Table S6). For the pair Cnx5–Cnx7, a factor of 3.6 ± 2.4 was calculated (Supplementary Fig. S2B; Suppementary Table S7) which highlights the reaction cascade: Cnx5 transfers the sulphur atom to Cnx7 but not to Cnx6 (compare Fig. 1). For comparison, all split LUC factors obtained herein are summarized in Table 1A. In order to substantiate these results with an independent *in vivo* approach, the interactions of both protein pairs were assayed with BiFC. The images in Fig. 2A and B indicate a clear interaction between Cnx6 and Cnx7, while Fig. 2C and D shows the limitations of BiFC. Comparing the sample (Fig. 2C) with its negative control (Fig. 2D; Supplementary Fig. S3) would hardly indicate an interaction between Cnx5 and Cnx7, thus necessitating a second independent interaction approach in addition to BiFC.

The C-terminus of the molybdopterin synthase small subunit is essential for interaction

The C-terminal region of the small subunit Cnx7 of MPT synthase is highly conserved among diverse species including the terminal double glycine motif which carries the sulphur atom to be transferred to the Moco intermediate cPMP (compare Fig. 1). The crystal structure of *E. coli* MPT synthase (Rudolph *et al*., 2001) revealed that the heterotetrameric complex has an elongated shape with the two large subunits forming a central dimer and the two small subunits being located at the opposite ends of the central dimer. The sulphur-carrying C-terminus of each small subunit inserts into a pocket of each large subunit, thus forming two probably independent active sites. If the terminal double glycine motif was changed by replacing either the last or the penultimate glycine, activities of *E. coli* and human MPT synthase were impaired (Hänzelmann *et al*., 2002). To

Table 1. (A) Split LUC factors of protein–protein interaction studies of the Moco biosynthesis pathway. (B) Direct comparison of split LUC luminescence of Cnx7 double glycine motif mutants with the wild type related to Cnx7 interaction

A

First protein (NLUC)	Second protein (CLUC)	Negative control	Split LUC factor[a]
Cnx6–NLUC	CLUC–Cnx6	StrepII–NLUC	12.0 ± 3.0
Cnx6–NLUC	CLUC–Cnx7	CFP–NLUC	11.9 ± 4.5
Cnx6–NLUC	Cnx7–CLUC	CFP–NLUC	3.3 ± 1.4
NLUC–Cnx5	CLUC–Cnx6	NLUC–CFP	1.3 ± 1.9
NLUC–Cnx5	CLUC–Cnx7	NLUC–CFP	3.6 ± 2.4
Cnx1–NLUC	CLUC–Cnx6	H2B–NLUC	1.5 ± 0.9
Cnx1–NLUC	CLUC–Cnx7	H2B–NLUC	0.3 ± 0.7
NLUC–Cnx6	Cnx1G–CLUC	StrepII–NLUC	1.6 ± 0.8
NLUC–Cnx6	Cnx1E–CLUC	StrepII–NLUC	3.3 ± 1.5
Cnx3–NLUC	Cnx2–CLUC	Cnx3TS–CLUC	1.4 ± 1.1

B

Studied protein pair (mutant)		Compared protein pair (wild type)		Reference value[b]	Resulting split LUC factor[c]
Cnx6–NLUC	CLUC–Cnx7AA	Cnx6–NLUC	CLUC–Cnx7	0.9 ± 0.8	10.8
	CLUC–Cnx7FG		CLUC–Cnx7	0.7 ± 1.0	7.9
	CLUC–Cnx7EG		CLUC–Cnx7	0.5 ± 1.7	5.6

[a] All split LUC factors include abundance adjustment.
[b] The reference value results from the direct comparison of the protein pair (wild type versus mutant) which was used for calculation of the resulting split LUC factor[c] based on Cnx6–NLUC with CLUC–Cnx7 (factor 11.9; compare part A).

investigate, if this functional impairment is accompanied by a disturbance of protein interaction between the subunits, the Split-LUC complementation assay was used. Therefore, different variants of the C-terminus of the small subunit Cnx7 of MPT synthase were tested for interaction with the large subunit Cnx6 (as Cnx6–NLUC). At first the N-terminus of Cnx7 was fused with CLUC (forming CLUC–Cnx7) in order to keep the functionally important Cnx7 C-terminus free for protein interaction, thus giving an interaction factor of 11.9 ± 4.5 (Table 1A). When, however, the C-terminus of Cnx7 was fused to CLUC (forming Cnx7–CLUC) thus blocking it, the interaction factor decreased to 3.3 ± 1.4 (Table 1A). Then the variants Cnx7AA, Cnx7FG, and Cnx7EG (always as CLUC–Cnx7 with a free C-terminus) were generated, transiently expressed in *N. benthamiana*, and directly compared with wild-type Cnx7. Table 1B shows that exchanging the two terminal glycines of Cnx7 each with another small amino acid (alanine) did not impair the interaction of Cnx7 with Cnx6 (interaction factor 10.8). However, replacing the penultimate glycine with a large amino acid – either aromatic (phenylalanine) or charged (glutamic acid) – reduced the interaction factor to 7.9 and 5.6, respectively.

Protein interaction between molybdopterin synthase and molybdenum insertase Cnx1

The conversion of the Moco intermediate cPMP to MPT proceeds on the large subunits (Cnx6) of MPT synthase, while its small subunits (Cnx7) supply sulphur atoms for insertion into cPMP. Subsequently, the MPT molecule formed on Cnx6 has to be transferred to molybdenum insertase Cnx1 which catalyses the final steps of Moco formation (compare Fig. 1). MPT, however, is short lived (Wuebbens and Rajagopalan 1993), oxygen sensitive, and unstable. Therefore, it was assumed that a multiprotein complex consisting of MPT synthase and molybdenum insertase Cnx1 would facilitate a protected product–substrate flow (Mendel and Bittner, 2006). Cnx1 is a two-domain protein. As expected, the full-length protein as well as its separately expressed subdomains were found to localize to the cytoplasm (data not shown). If Cnx1 undergoes protein contact with MPT synthase, this is supposed to happen between Cnx1 and Cnx6 because MPT is formed on the latter. Therefore, using the BiFC approach Venus^{N173} was fused to the N-terminus of Cnx1 (Venus^{N173}–Cnx1), and combined with the super cyan fluorescent protein SCFP^{C155}–Cnx6. Three days after Rhizobium-infiltration, bright fluorescence was observed with a spectral signature typical of this BiFC (Fig. 2E, F; Supplementary Fig. S3 at *JXB* online). Using the split LUC assay with the combination of Cnx1–NLUC and CLUC–Cnx6, an interaction factor of only 1.5 ± 0.9 was calculated (Table 1A). Also the small subunit of MPT synthase (Cnx7) was tested for interaction with Cnx1, but its split LUC factor was even lower (0.3). A split LUC factor <1.0 illustrates an accidental contact of the proteins studied. Obviously, Cnx1 and Cnx7 are kept apart by such a long distance where reconstitution of the LUC termini is impossible. The protein causing this steric hindrance could be Cnx6, as it interacts with both Cnx1 and Cnx7 simultaneously.

Protein contact between Cnx6 and the domains of molybdenum insertase Cnx1

Next the contact site on Cnx1 through which it interacts with Cnx6 was studied. Cnx1 (71.3 kDa) consists of an N-terminal domain named the E-domain (Cnx1E,

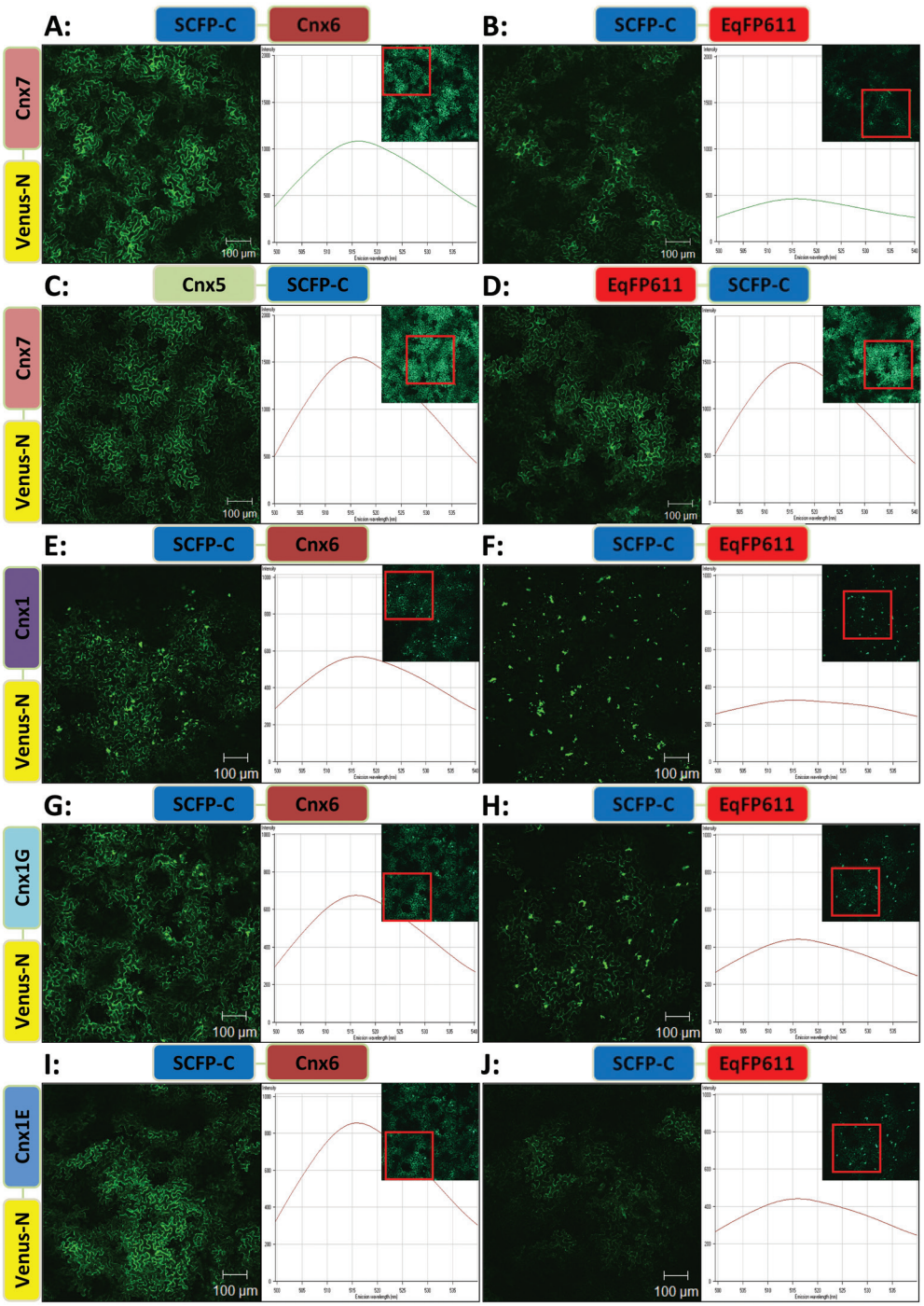

Fig. 2. Localization and visualization of protein–protein interactions in the Moco biosynthetic pathway via bimolecular fluorescence complementation (BiFC). Protein–reporter fusion constructs (symbolized within the single pictures as boxes coloured in the same colour code used throughout this paper) were analysed by confocal laser scanning microscopy after transferring the gene constructs via *Rhizobium* infiltration in *N. benthamiana*. Shown are representative pictures from 5–10 leaf discs of 2–3 plants. The fluorescence signal taken in the channel mode of the cLSM-510META is shown as well as its spectral signature (500–540 nm; peak at 515 nm) detected semi-quantitatively in the lambda mode by choosing the most fluorescing quarter of the recorded picture (see red box in the small lambda picture). BiFC pictures of the different protein–protein interactions and their respective negative controls were taken with identical settings. Therefore, the intensities in the lambda mode are comparable for each pair (i.e. between graphs in the same horizontal line). However, intensities between different pairs are not comparable because of different expression levels. (A–J) BiFC images of different protein–protein interactions within the cytoplasmic parts of the Moco biosynthetic pathway (A, C, E, G, I) as well as their respective negative controls (B, D, F, H, J). (A) MPT synthase proteins Cnx6 and Cnx7; (C) Cnx7 and MPT synthase sulphurase Cnx5; MPT synthase protein Cnx6 with Mo insertase Cnx1 (E) as well as domains Cnx1G (G) and Cnx1E (I). BiFC studies with Cnx1 (E, F) and Cnx1G (G, H) shows the tendency to form distinct fluorescing aggregates with interacting protein and negative control proteins, respectively.

47.0 kDa) and a C-terminal domain named the G-domain (Cnx1G, 23.0 kDa) connected by a short linker (Stallmeyer *et al*., 1995; Schwarz *et al*., 2000). Previously, Llamas *et al*. (2006) found that Cnx1G binds MPT and adenylates it. The formed MPT-AMP is transferred to the E-domain where the adenylate is cleaved and Mo inserted (compare Fig. 1). Hence it was reasonable to assume that the contact between Cnx1 and Cnx6 should be mediated by the G-domain. Therefore, the Venus moiety was fused to the N- and C-terminus, respectively, of Cnx1G and co-transferred with the correct counterpart of Cnx6. Surprisingly, 3 d after *Rhizobium* infiltration, the BiFC signal of the interaction partners was only slightly stronger than that of the respective negative control (compare Fig. 2E and F and the intensities of the spectral signatures). Moreover, Cnx1G has the tendency to form aggregates of high fluorescence intensity when fused at the N-terminus to the fluorochrome, as shown for the complete Cnx1 and even in the negative controls (Fig. 2E–H).

As a next step, the Cnx1E-domain was also tested for *in vivo* fluorescence complementation with Cnx6. All possible orientations of the fluorochrome were fused to the E-domain and combined with the compatible Cnx6 fusion constructs. Three days after *Rhizobium* infiltration, a strong BiFC fluorescence was observed in the cytoplasm in all transformations tested. Using the respective negative controls as the basis, Cnx1E (Venus^{N173}–Cnx1E) plus Cnx6 (SCFP^{C155}–Cnx6) gave a stronger BiFC signal than the Cnx1G-domain and full-length Cnx1 protein, respectively (compare Fig. 2E–J; Supplementary Fig. S3 at *JXB* online). This overall impression could be verified using the lambda signature of the fluorochromes. Moreover, Cnx1E showed no aggregates. When quantifying these protein combinations with the split LUC approach, a similar picture was obtained. The single domains (Cnx1G–CLUC and Cnx1E–CLUC, respectively) in combination with NLUC–Cnx6 gave a split LUC factor of 1.6 ± 0.8 for the G-domain and a factor of 3.3 ± 1.5 for the E-domain (Table 1A).

Cross-linking and label transfer between molybdopterin synthase and molybdenum insertase

As the E-domain of molybdenum insertase Cnx1 gave stronger interactions with MPT synthase than its G-domain (in both the BiFC and the split LUC assays), this result was also checked *in vitro* using the tool ‘cross-linking and label transfer’ (Layer *et al*., 2007). Here, two interacting proteins become cross-linked using a tri-functional photoactivatable linker. The third function of this linker is biotin. At first, the linker is covalently coupled to protein A; thus protein A can be detected by its biotin label. When protein B gets as near as 1 nm, it becomes cross-linked to protein A. This link can be broken by reductant in such a way that the biotin label leaves protein A and becomes bound to protein B. Now protein B can be detected by its biotin label. Using this technique, it could be determined whether Cnx6 can be cross-linked to a domain of Cnx1. Protein Cnx6 was labelled with the tri-functional cross-linker Mts–Atf–biotin and incubated with Cnx1E and Cnx1G, respectively, in order to see to what domain the biotin label was transferred. As a control, BSA was used as the recipient for the biotin label. Figure 3 shows that only the E-domain became labelled (arrow), but neither Cnx1G nor BSA showed any interaction. Likewise, no biotin transfer could be observed if instead of Cnx6 the G-domain was biotin labelled and incubated with Cnx6 as recipient (Fig. 3), while labelling of Cnx1E and biotin transfer to Cnx6 was positive (data not shown). BiFC and split LUC seem to be more sensitive than *in vitro* cross-linking as the latter did not detect the interaction with the G-domain while the *in vivo* approaches still gave a weak interaction signal.

Cnx2 and Cnx3 undergo protein contact inside mitochondria

Proteins Cnx2 and Cnx3 catalyse the first step of Moco biosynthesis (compare Fig. 1). By immunoblot analysis it was previously found that Cnx2 and Cnx3 localize to mitochondria (Teschner *et al*., 2010). Cellular localization of the proteins was analysed by fusing the N- terminal targeting signals (amino acids 1–50 and 1–43 for Cnx2 and Cnx3, respectively) in front of Venus fluorescence protein. The laser scanning microscopy picture showed a punctuated fluorescence signal (Fig. 4A, B) which could be counterstained using the mitochondrial pIVD145-eqFP611 construct displayed in blue (Wiedenmann *et al*., 2002; Forner and Binder, 2007). In the merged pictures, co-localization is indicated by the resulting white colour.

Moreover, it was of interest to determine whether Cnx2 and Cnx3 undergo protein interaction in the course of their functioning inside mitochondria. Only C-terminal fusions of the full-length proteins were used because of the need for a freely accessible N-terminal targeting signal, fused to the N- or C-terminal part of Venus and SCFP, respectively (Fig. 4C, D). The results not only confirm that both Moco biosynthesis proteins are localized in the mitochondria, but they also demonstrate that Cnx2 and Cnx3 undergo protein interaction within this organelle. When testing the interaction of these proteins with the split LUC approach, the overall protein expression was weak (Table 1A). The interaction takes place within the mitochondria, which makes it difficult to detect the luminescence.

Discussion

Protein fragment complementation assays allow investigation of protein–protein interactions *in vivo* in the original subcellular compartments of the cell. While the BiFC approach helps to answer the question of where in the cell an interaction between two proteins takes place, the split LUC approach allowed measurement of the strength of such interactions. The unhindered interaction of the studied proteins is guaranteed by the peptide linkers used to separate the reporter fragment and the studied protein. These linkers (11–29 amino

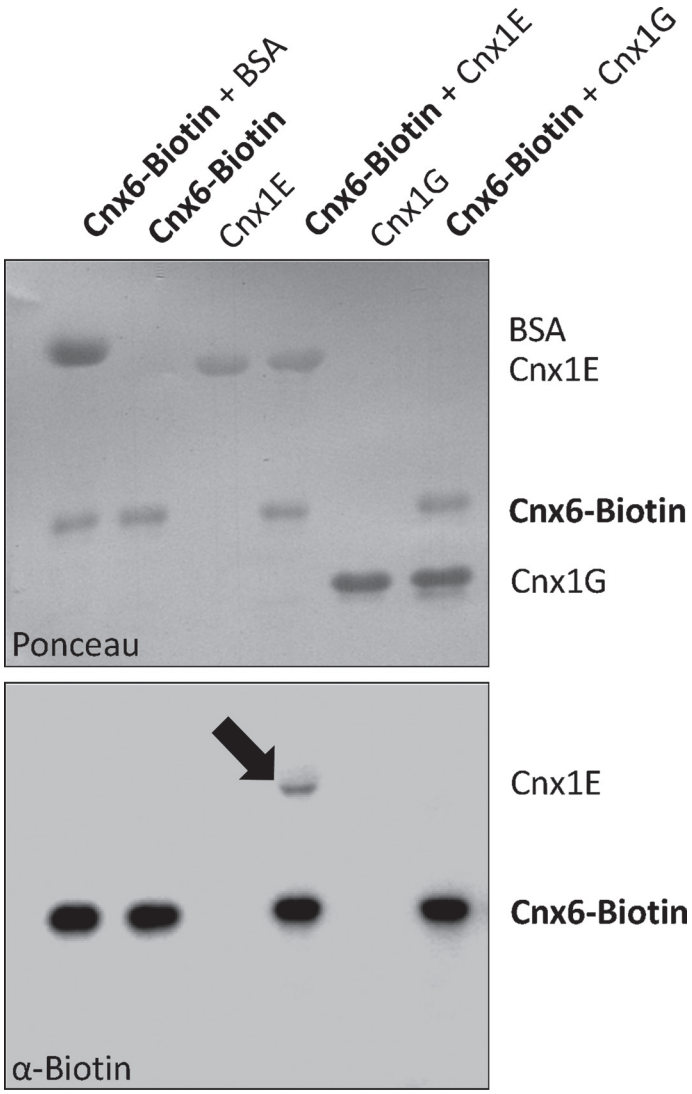

Fig. 3. Label transfer with Cnx6 as prey protein and Cnx1E and Cnx1G as bait proteins. Labelled proteins (shown in bold) were incubated with equimolar amounts of putative binding partners and irradiated with UV light to initiate cross-linking and label transfer. The top panel shows the Ponceau-stained SDS–gel after blotting, and the bottom panel shows the immunoblotted samples with horseradish–streptavidin conjugate (α-biotin); the arrow marks the label transfer.

acids long) include the amino acids resulting from the translated *att*B sites and, in the split LUC vectors, additionally the highly flexible -GGSG- peptide known from the work of Cheung *et al*. (2012).

With the exception of peroxisomal sulphite oxidase (Nowak *et al*., 2004) and mitochondrial amide oxime reducing component (Havemeyer *et al*., 2006; unpublished data), all remaining plant Mo-enzymes are localized in the cytoplasm. Also Moco biosynthesis was assumed to proceed in the cytoplasm, and Cnx1, as the enzyme catalysing the last step of Moco biosynthesis, was shown to bind to actin filaments (Schwarz *et al*., 2000). Further, the existence of a multienzyme complex was discussed that should facilitate the fast and protected product–substrate flow of labile Moco intermediates (Mendel and Bittner, 2006). The BiFC results showed that the MPT synthase (catalysing step 2 of Moco biosynthesis) and Cnx1 (catalysing steps 3 and 4) are located in the cytoplasm and undergo tight protein–protein interaction. Thus it can be assumed that MPT synthase directly sequesters the newly formed MPT to Cnx1 where it becomes converted to mature Moco. How many proteins form this multimeric cytosolic complex? MPT synthase is heterotetrameric, while for Cnx1 its oligomerization state *in situ* is not clear. Under *in vitro* conditions, Cnx1G forms trimers and Cnx1E dimers (Schwarz *et al*., 1997), whereas holo-Cnx1 shows an ambiguous behaviour depending on the conditions. As MPT synthase possesses two clearly separated active sites on opposite ends of its structure (compare Fig. 1) one may speculate that altogether two molecules of Cnx1 are necessary to take over the newly formed MPT, one molecule of Cnx1 at each end of MPT synthase. Thus at least six proteins might build this Moco biosynthesis complex. Figure 5 summarizes the interaction strengths measured for this complex. One has to consider, however, that such a complex is dynamic as the small subunit (Cnx7) of MPT synthase has to go on and off in order to become recharged with sulphur by Cnx5 (compare Fig. 1) and one may speculate that the core complex is formed by Cnx6 and Cnx1.

Recently mitochondria were biochemically shown to harbour the first step of Moco biosynthesis and to export the Moco intermediate cPMP to the cytoplasm (Teschner *et al*., 2010) where it becomes further processed to MPT and Moco. Here these data were confirmed by localization experiments using fluorescence labelled proteins and *in vivo* protein–protein interaction studies. Likewise, the Mo enzymes as users of Moco are synthesized and assembled in the cytoplasm. Comparing the stability of the two Moco intermediates MPT and cPMP, MPT is more labile (Wuebbens and Rajagopalan, 1993). Clearly, the channelling of MPT within a multienzyme complex would protect and stabilize this fragile compound. On the other hand, cPMP as the first Moco intermediate seems to be stable enough to survive its export from the mitochondria.

Escherichia coli MPT synthase was shown to have an elongated shape, with the two large subunits forming a central dimer and the two small subunits being located at opposite ends of the central dimer (Rudolph *et al*., 2001). Utilizing the split LUC approach to compare binding strength directly between Cnc6/Cnx6 homodimers and Cnx6/Cnx7 heterodimers, it turned out that both were of the same strength, with the highest interaction factor measured in the present system (factor 12). On interaction of Cnx7 with Cnx6, Cnx7 inserts its C-terminus with the conserved double glycine motif deeply into a pocket of Cnx6. Replacing the last or the penultimate glycine of *E. coli* and human MPT synthase drastically impaired their enzymatic activities (Hänzelmann *et al*., 2002). Using the split LUC approach, an attempt was first made to dissect interaction from functionality of MPT synthase. Replacing the two highly conserved terminal glycines of Cnx7 with another small amino acid (alanine)

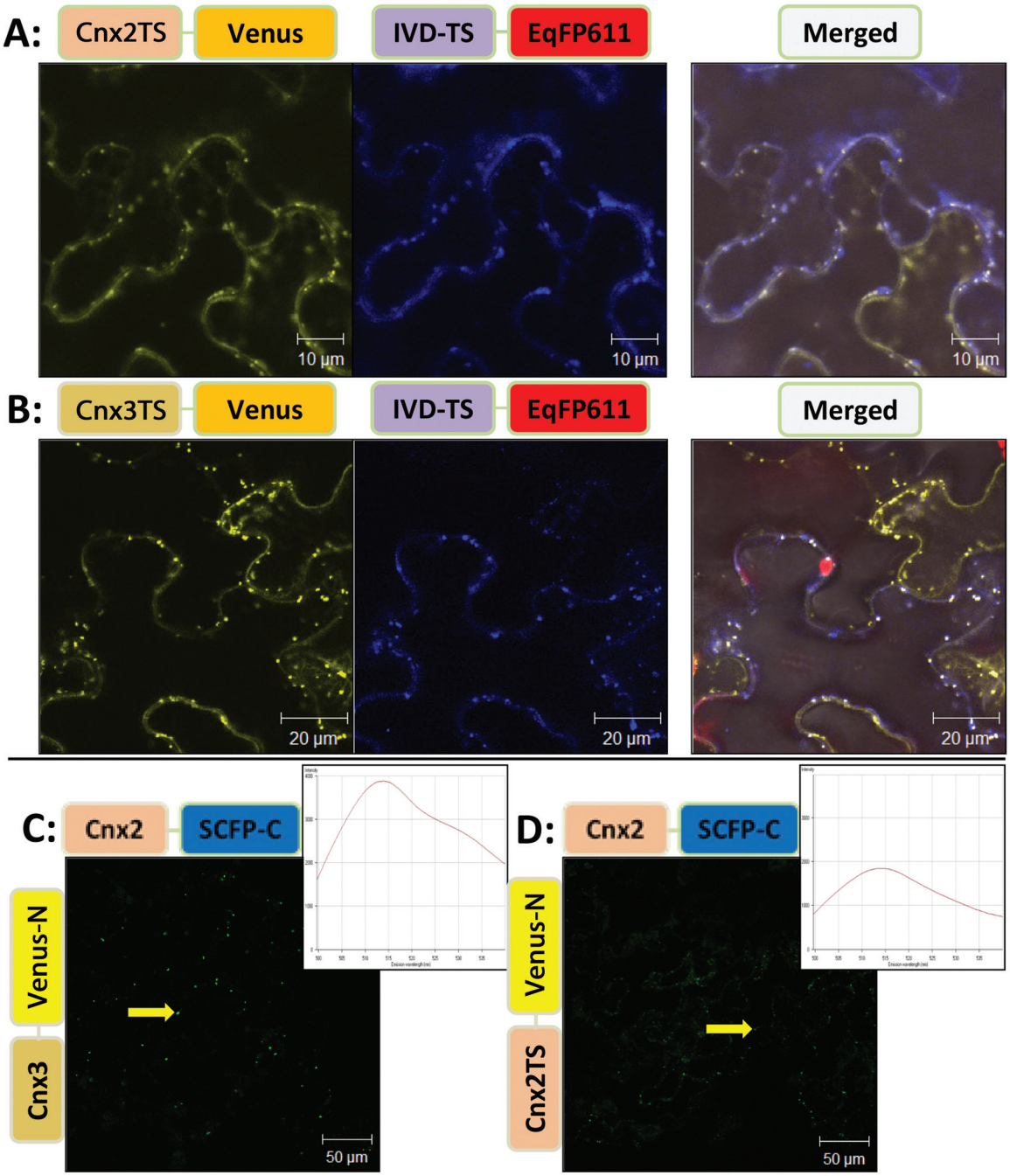

Fig. 4. Localization and BiFC interaction studies of the first step in Moco biosynthesis in mitochondria. (A, B) Localization of Cnx2 and Cnx3 was achieved by fusing the N-terminal targeting signal (amino acids 1–50 and 1–43 for Cnx2 and Cnx3, respectively) in front of Venus (left picture). Co-localization of a mitochondrial marker (pIVD145-eqFP611; Forner and Binder, 2007) is shown in the central picture (blue). The right-hand picture is the merged version indicating co-localization of the proteins in white. (C) Representative BiFC signal of the interaction between Cnx2 and Cnx3 in the mitochondria and (D) the specific negative control. The signal is taken in the channel mode of the cLSM-510META by using the same settings. The spectral signature (500–540 nm; peak at 515 nm) was monitored semi-quantitatively in the lambda mode by choosing the most strongly fluorescing mitochondrion of the recorded picture (see yellow arrow).

did not change the interaction of Cnx7 with Cnx6, while previous studies showed that this replacement (GG→AA) led to a complete loss of activity in human MPT synthase (Hänzelmann *et al.*, 2002). When, however, the penultimate glycine was replaced with a large amino acid – either aromatic (phenylalanine) or charged (glutamic acid) – the interaction between the subunits was also reduced, obviously because of steric hindrance.

The results of the BiFC and split LUC approaches became substantiated when one checks them with an independent approach not involving fluorescence or luminescence of protein moieties. In the present case, this independent approach

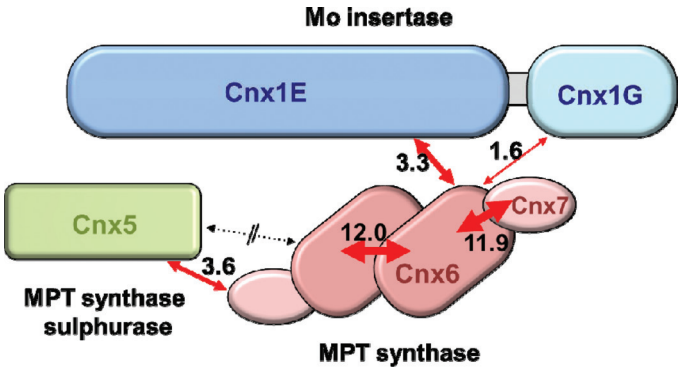

Fig. 5. Summary scheme of protein interactions in the cytosolic steps of Moco biosynthesis. The strengths of interactions are indicated by the interaction factors (given in arbitrary units) as well as by the thickness of the respective arrows.

was *in vitro* cross-linking and label transfer. The combination of both approaches served as a dissecting tool to narrow down the contact sites within the Moco biosynthsis complex. A surprising result of the split LUC experiments was that the pair Cnx1E/Cnx6 had a stronger interaction factor than the pair Cnx1G/Cnx6. This was unexpected because the sequence of reactions catalysed by Cnx1 starts on its G-domain that binds and adenylates MPT. Subsequently, MPT-AMP is transferred to the E-domain where the adenylate is cleaved and Mo is inserted (Llamas *et al.*, 2006). The newly formed Moco is stabilized by Cnx1 until it is distributed to the final users (Kuper *et al.*, 2004). Hence it was reasonable to assume that the contact between Cnx1 and Cnx6 should be mediated by the G-domain. However, already our BiFC findings identified the E-domain as interacting more efficiently with Cnx6. Also, in an independent *in vivo* approach, the Cnx1E-domain was co-purified with overexpressed and tagged Cnx6 (data not shown), thus suggesting that the interaction between both proteins is of a tighter nature. These *in vivo* results are consistent with the *in vitro* data of protein cross-linking and label transfer. Also here the contact mediator between Cnx1 and Cnx6 turned out to be the E-domain of Cnx1. How can these results be explained? Cnx1 is a two-domain protein (71.3 kDa) consisting of an N-terminal E-domain (45.0 kDa) and a C-terminal G-domain (26.5 kDa) connected by a 22 amino acid linker (Stallmeyer *et al.*, 1995). Based on the observed MPT binding to both domains of Cnx1, a substrate binding common to both domains was assumed (Stallmeyer *et al.*, 1995; Llamas *et al.*, 2006). Structural analysis of the large and very elongated E-domain of gephyrin (equivalent the mammalian homologue of Cnx1) (Sola *et al.*, 2004; Fritschy *et al.*, 2008) showed that it forms four distinct subdomains. Most remarkably, one of these subdomains turned out to be structurally similar to the G-domain, i.e. Cnx1 principally possesses two G-domains: a separate C-terminal G-domain and another G-like subdomain embedded within the E-domain. These data suggest a common binding fold for MPT in both domains of Cnx1. Indeed, earlier biochemical characterizations of the Cnx1 domains had revealed that both domains are able to bind MPT although with different affinities (Schwarz *et al.*, 1997). Thus steric reasons could account for the observation that MPT synthase (Cnx6/Cnx7) makes easier contact with the E-domain as compared with the G-domain. Supportive evidence for this assumption comes from structural comparisons between Cnx1 and its mammalian homologue gephyrin – it was suggested that gephyrin occurs as a trimer and forms a propeller-like structure with the small G-domain trimer hidden in the centre and the longer E-domains sticking out of the surface as the 'propeller blades' (Sola *et al.*, 2004; Fritschy *et al.*, 2008). For gephyrin in neuronal cells, this trimerization feature is the structural basis for its ability to form a hexagonal lattice for the anchoring of receptors and other proteins. Perhaps this feature is also the reason for the tendency of the G-domain constructs to form aggregates when expressed in plant cells.

In summary, the data presented here allow the first draft of an interaction matrix for proteins within the pathway of synthesis and allocation of Moco to be outlined. Clearly, the cytosol is not a 'bag of proteins and metabolites that freely swirl around', but is structured through micro-compartmentalization. In this context, the cytoskeleton binding of the molybdenum insertase Cnx1 (Schwarz *et al.*, 2000) might be of importance. Moco biosynthesis and allocation emerge as a good example to illustrate such a micro-compartmentalization: channelling of fragile intermediates and allocating the final labile product in a protected way is achieved through a series of direct protein interactions. Further experiments are in progress to provide more detail on the interaction matrix of proteins downstream of Moco biosynthesis in higher plants.

Supplementary data

Supplementary data are available at *JXB* online.

Figure S1. Localization of Cnx6, Cnx7, and Cnx5.
Figure S2. Split LUC study of Cnx5/Cnx6 and Cnx5/Cnx7.
Figure S3. Abundance controls of BiFC studies.
Table S1. GATEWAY destination vectors.
Table S2. Peptide linkers used in fusion constructs.
Table S3. PCR primers.
Table S4. GATEWAY entry vectors.
Table S5. GATEWAY expression vectors.
Table S6. Split LUC factor calculation (Cnx5/Cnx6).
Table S7. Split LUC factor calculation (Cnx5/Cnx7).

Acknowledgements

This work was supported by a grant from the Deutsche Forschungsgemeinschaft (Me1266/14–5). We are grateful to Marion Kay and the students Carolin Mahler, Janine Strehmel, Yasemin Sömer, Michael Reusche, Anna Börger, Robert Bittorf, Anna-Lena Krützfeldt, and Frederike Imbusch for excellent technical work in our lab. We thank Professor Binder (Ulm, Germany) and VIB (www.psb.ugent.be) for kindly providing vectors pIVD145-eqFP611-pBI121, and pK7WG2, respectively.

References

Bittner F, Mendel RR. 2010. Cell biology of molybdenum. In: Hell R, Mendel RR, eds. *Cell biology of metals and nutrients, Plant Cell Monographs* , Vo. **17**. Berlin: Springer, 19–143.

Bradford MM. 1976. A rapid and sensitive method for the quantitation of microgram quantities of protein utilizing the principle of protein–dye binding. *Analytical Biochemistry* **72,** 248–54.

Chen H, Zou Y, Shang Y, Lin H, Wang Y, Cai R, Tang X, Zhou JM. 2008. Firefly luciferase complementation imaging assay for protein–protein interactions in plants. *Plant Physiology* **146,** 368–376.

Cheung LS-L, Kanwar M, Ostermeier M, Konstantopoulos K. 2012. A Hot-spot motif characterizes the interface between a designed ankyrin-repeat protein and its target ligand. *Biophysical Journal* **102,** 407–416.

Forner J, Binder S. 2007. The red fluorescent protein eqFP611: application in subcellular localization studies in higher plants. *BMC Plant Biology* **7,** 28.

Fritschy JM, Harvey RJ, Schwarz G. 2008. Gephyrin: where do we stand, where do we go? *Trends in Neuroscience* **31,** 257–264.

Gehl C, Kaufholdt D, Hamisch D, Bikker R, Kudla J, Mendel RR, Hänsch R. 2011. Quantitative analysis of dynamic protein–protein interactions *in planta* by a floated-leaf luciferase complementation imaging (FLuCI) assay using binary Gateway vectors. *The Plant Journal* **67,** 542–543.

Gehl C, Waadt R, Kudla J, Mendel RR, Hänsch R. 2009. New GATEWAY vectors for high throughput analyses of protein–protein interactions by bimolecular fluorescence complementation. *Molecular Plant* **2,** 1051–1058.

Hänzelmann P, Schwarz G, Mendel RR. 2002. Functionality of alternative splice forms of the first enzymes involved in human molybdenum cofactor biosynthesis. *Journal of Biological Chemistry* **277,** 18303–18312.

Havemeyer A, Bittner F, Wollers S, Mendel RR, Kunze T, Clement B. 2006. Identification of the missing component in the mitochondrial benzamidoxime prodrug-converting system as a novel molybdenum enzyme. *Journal of Biological Chemistry* **281,** 34796–34802.

Jefferson RA, Kavanagh TA, Bevan MW. 1987. GUS fusions: β-glucuronidase as a sensitive and versatile gene fusion marker in higher plants. *EMBO Journal* **6,** 3901–3907.

Kerppola TK. 2008. Bimolecular fluorescence complementation (BiFC) analysis as a probe of protein interactions in living cells. *Annual Review of Biophysics* **37,** 465–487.

Kruse T, Gehl C, Geisler M, Lehrke M, Ringel P, Hallier S, Hänsch R, Mendel RR. 2010. Identification and biochemical characterization of molybdenum cofactor-binding proteins from *Arabidopsis thaliana*. *Journal of Biological Chemistry* **285,** 6623–6635.

Kuper J, Llamas A, Hecht HJ, Mendel RR, Schwarz G. 2004. Structure of the molybdopterin-bound Cnx1G domain links molybdenum and copper metabolism. *Nature* **430,** 803–806.

Layer G, Gaddam SA, Ayala-Castro CN, Ollagnier-de Choudens S, Lascoux D, Fontecave M, Outten FW. 2007. SufE transfers sulfur from SufS to SufB for iron–sulfur cluster assembly. *Journal of Biological Chemistry* **282,** 13342–13350.

Llamas A, Otte T, Multhaup G, Mendel RR, Schwarz G. 2006. The mechanism of nucleotide-assisted molybdenum insertion into molybdopterin. A novel route toward metal cofactor assembly. *Journal of Biological Chemistry* **281,** 18343–18350.

Luker KE, Smith MC, Luker GD, Gammon ST, Piwnica-Worms H, Piwnica-Worms D. 2004. Kinetics of regulated protein–protein interactions revealed with firefly luciferase complementation imaging in cells and living animals. *Proceedings of the National Academy of Sciences, USA* **101,** 12288–12293.

Matthies A, Rajagopalan KV, Mendel RR, Leimkuhler S. 2004. Evidence for the physiological role of a rhodanese-like protein for the biosynthesis of the molybdenum cofactor in humans. *Proceedings of the National Academy of Sciences, USA* **101,** 5946–5951.

Mendel RR, Bittner F. 2006. Cell biology of molybdenum. *Biochimica et Biophysica Acta* **1763,** 621–635.

Mendel RR, Kruse T. 2012. Cell biology of molybdenum in plants and humans. *Biochimica et Biophysica Acta* **1823,** 1568–1579.

Mendel RR, Schwarz G. 2011. Molybdenum cofactor biosynthesis in plants and humans. *Coordination Chemistry Reviews* **255,** 1145–1158.

Nowak K, Luniak N, Witt C, Wüstefeld Y, Wachter A, Mendel RR, Hänsch R. 2004. Peroxisomal localization of sulfite oxidase separates it from chloroplast-based sulfur assimilation. *Plant and Cell Physiology* **45,** 1889–1894.

Rudolph MJ, Wuebbens MM, Rajagopalan KV, Schindelin H. 2001. Crystal structure of molybdopterin synthase and its evolutionary relationship to ubiquitin activation. *Nature Structural Biology* **8,** 42–46.

Sambrook J, Russell DW. 2001. *Molecular cloning: a laboratory manual* . Cold Spring Harbor, NY: Cold Spring Harbor Laboratory Press.

Santamaria-Araujo JA, Fischer B, Otte T, Nimtz M, Mendel RR, Wray V, Schwarz G. 2004. The tetrahydropyranopterin structure of the sulfur-free and metal-free molybdenum cofactor precursor. *Journal of Biological Chemistry* **279,** 15994–15999.

Schwarz G, Boxer DH, Mendel RR. 1997. Molybdenum cofactor biosynthesis. The plant protein Cnx1 binds molybdopterin with high affinity. *Journal of Biological Chemistry* **272,** 26811–2684.

Schwarz G, Mendel RR, Ribbe MW. 2009. Molybdenum cofactors, enzymes and pathways. *Nature* **460,** 839–847.

Schwarz G, Mendel RR. 2006. Molybdenum cofactor biosynthesis and molybdenum enzymes. *Annual Review of Plant Biology* **57,** 623–647.

Schwarz G, Schulze J, Bittner F, Eilers T, Kuper J, Bollmann G, Nerlich A, Brinkmann H, Mendel RR. 2000. The molybdenum cofactor biosynthetic protein Cnx1 complements molybdate-repairable mutants, transfers molybdenum to the metal binding pterin, and is associated with the cytoskeleton. *The Plant Cell* **12,** 2455–2472.

Sola M, Bavro VN, Timmins J, *et al.* 2004. Structural basis of dynamic glycine receptor clustering by gephyrin. *EMBO Journal* **23,** 2510–2519.

Stallmeyer B, Nerlich A, Schiemann J, Brinkmann H, Mendel RR. 1995. Molybdenum co-factor biosynthesis: the *Arabidopsis thaliana* cDNA cnx1 encodes a multifunctional two-domain protein

homologous to a mammalian neuroprotein, the insect protein Cinnamon and three *Escherichia coli* proteins. *The Plant Journal* **8,** 751–62.

Teschner J, Lachmann N, Schulze J, Geisler M, Selbach K, Santamaria-Araujo J, Balk J, Mendel RR, Bittner F. 2010. A novel role for Arabidopsis mitochondrial ABC transporter ATM3 in molybdenum cofactor biosynthesis. *The Plant Cell* **22,** 468–480.

Wiedenmann J, Schenk A, Rocker C, Girod A, Spindler KD, Nienhaus GU. 2002. A far-red fluorescent protein with fast maturation and reduced oligomerization tendency from *Entacmaea quadricolor* (Anthozoa, Actinaria). *Proceedings of the National Academy of Sciences, USA* **99,** 11646–11651.

Wuebbens MM, Rajagopalan KV. 1993. Structural characterization of a molybdopterin precursor. *Journal of Biological Chemistry* **268,** 13493–13498.